VARIABLE SPEED CONSTANT FREQUENCY POWER CONVERSION WITH A SWITCHED RELUCTANCE MACHINE

* Geunhie Rim and ** R.Krishnan

* Power Electronics Research Lab.
Korea Electrotechnology Research Institute
Chang-Won Gyung-Nam, Korea

** Dept. of Electrical Engineering
VPI & SU, Blacksburg, VA 24061

Abstract

A converter topology which is capable of four-quadrant (motoring and generation) operation is proposed for the variable speed constant frequency(hereafter referred as VSCF) power conversion scheme. The new converter topology for the VSCF power conversion scheme is made of two functional stages. One is converting stage which consists of six switches and six diodes and it interfaces a three-phase 60Hz ac supply and a single-phase variable-frequency ac source. The other is the commutating stage though which each phase-winding is energized.

I. Introduction

The overall power conversion scheme is shown in Figure 1. The scheme works for both generating and motoring operations. In the generator mode, the shaft is driven by a prime mover. The electro-magnetic torque developed in the generator (when it delivers power) opposes the torque of the prime mover. The losses due to the copper and iron core, friction and converter causes the difference between these two torques. In a motor the electromagnetic torque developed in the machine except the losses is delivered to the shaft which drives the mechanical load. In this scheme, the SRM is directly connected to the shaft of a prime mover which has a variable-speed power such as an aircraft starter-generator. In the experimental set-up, a dc machine is mechanically coupled to the SRM. For generation the dc machine provides the variable-speed power to the system as a prime mover, and for motoring it takes power from the system as a load. The SRM rotor position is obtained from an optical encoder which is installed on the rotor shaft. The machine interfaces to the three phase mains through the proposed converter. During motoring, the converter acts as an inverter and drives the SRM as a motor. For generating operation, the power converter provides excitation to the SRM and extracts the resulting generated power directly to the ac mains.

II. Topology

The new converter topology for the VSCF power conversion scheme is made of two functional stages. One is converting stage which consists of six switches and six diodes and it interfaces a three-phase 60 Hz ac supply and a single-phase variable-frequency ac source. The other is the commutating stage through which each phase-winding is energized.

The functions of these converters for SRM drives may be briefly described as follows. When the rotor is appropriately positioned with respect to the stator, unidirectional current pulses are applied across the phase windings to energize. If a desired current is commanded, a rapid response is needed for the demanded phase current level, which requires a two quadrant power converter which is capable of applying equal positive and negative phase voltage when necessary. This is done usually by reversing the current direction of the phase winding through feedback diodes, on the contrary, the proposed converter keeps the source current direction, and changes the voltage polarity instead. Most of the SRM drives(the rectifier-capacitor source) except battery-source cases can not directly feed the energy to the source due to the diode bridge and the current limitation of the electrolytic power-capacitor, thus only limited amount of returned energy is stored in the capacitors and reused. As a

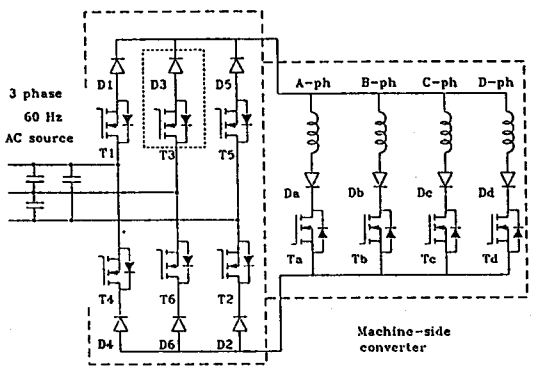

Figure 1. The proposed converter configuration

result, an extra circuit such as dump resistor across the capacitor may be required to limit the voltage rise in the dc link, this resulting in a low efficiency. In such cases the reversed current affects the life-time of the capacitor due to the frequent charging and discharging actions. However the new converter can return the power from the machine to the source directly without any limitations and eliminates the dc link capacitor. The elimination of dc link capacitor resulting in cost savings and enhancement of the reliability of the scheme and increasing the power density of the scheme due to lower weight.

III. Theoretical and experimental results

A. Theoretical results

The voltage across a phase winding is closely associated with the flux linkage(of a winding) which varies cyclically with rotor position, θ and phase current i. From the equivalent circuit for SRM phase winding shown in Figure 2(a), the general voltage equation for a phase winding is given by

$$\pm v_{dc} = iR_e + \frac{d\Psi(\theta,i)}{dt} \quad (1)$$
$$+ \text{ nonlinear circuit-component voltage-drop}$$
$$= iR_e + L(\theta,i)\frac{di}{dt} + i\frac{dL(\theta,i)}{dt} - M(\theta,i)\frac{di}{dt} \quad (2)$$
$$+ \text{ nonlinear circuit-component voltage-drop}$$

where, R_e is the circuit equivalent resistance including winding resistance(R_w), M is the mutual inductance due to coupling between phases, L is self inductance.

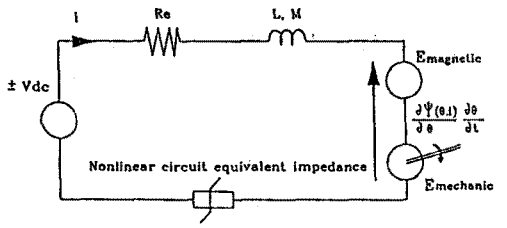

(a) Equivalent circuit of a phase winding

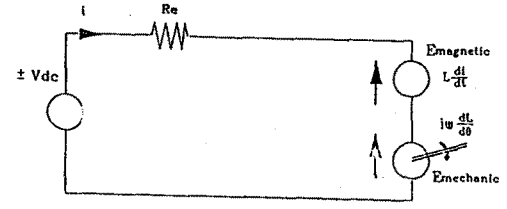

(b) Simplified equivalent circuit

Figure 2. Equivalent circuit of a phase winding

Neglecting the nonlinear circuit-component voltage drop, the circuit resistance except winding resistance, and assuming self inductance L in independent of current, the equation is given by

$$\pm v_{dc} = \frac{d\Psi(\theta,i)}{dt} + iR_w \quad (3)$$
$$= L\frac{di}{dt} + i\frac{dL}{dt} + iR_w \quad (4)$$
$$= L\frac{di}{dt} + i\frac{dL}{d\theta}\frac{d\theta}{dt} + iR_w \quad (5)$$
$$= L\frac{di}{dt} + i\frac{dL}{d\theta}\omega + iR_w \quad (6)$$

where, $\omega = d\theta/dt$, the rotational angular speed. Therefore the equivalent circuit diagram becomes as shown in Figure 2(b). The instantaneous electric power to a phase winding is given by

$$P_W = \pm v_{dc} i \quad (7)$$
$$= Li\frac{di}{dt} + i^2\omega\frac{dL}{d\theta} + i^2R_w \quad (8)$$
$$= \frac{d}{dt}(\frac{1}{2}Li^2) + \frac{1}{2}i^2\omega\frac{dL}{d\theta} + i^2R_w \quad (9)$$
$$= P_{Wmagetic} + P_{Wmechanic} + P_{Wcopper} \quad (10)$$

The first term of the equation is the variation of the stored magnetic field-energy in a phase winding, the last term stands for the winding copper-loss. The term in the middle of the equation represents the mechanical power output and it may be expressed alternatively as

$$P_{Wmechnic} = T_e\omega \quad (11)$$

where T_e is the electromagnetic torque. In motoring operation, T_e is positive in polarity, but in generation mode it becomes negative. It implies that if mechanical power is externally supplied in the generation mode, the machine can generate electric power. The mechanical equations describing the interactions between the load torque T_l and the electromagnetic torque is given by

$$J\frac{d\omega}{dt} + B\omega = T_e - T_l \quad (12)$$

$$\frac{d\theta}{dt} = \omega \quad (13)$$

where J is the moment of inertia, and B is the coefficient of viscous friction. Flux linkage in each phase and rotor position are obtained by solving the differential equations (3), (12) and (13) using numerical integration. Since flux linkage and rotor position are known, the phase current can be found from the $\Psi(\theta,i)$ data.

The predicted results of the scheme in the steady state are obtained using Backward-Euler method for the solution of differential equations. The results shown in Figure 3 includes phase-voltage, line-current and instantaneous power for ac source. The front-end converter is basically phase-controllable. Therefore, the current can flow at any phase

of the source voltage. The phase relationship between the phase voltage and current shown in the results is set at $\alpha = 0°$, similar to a thyristor-based phase-controlled rectifier. Dc link voltage is maximized at the activation angle. The instantaneous dc link power(P_o) and shaft-power(P_i) are determined by

$$P_o = \frac{1}{N}\sum_{i=0}^{N-1} v_a(t_i)i_a(t_i) + v_b(t_i)i_b(t_i) + v_c(t_i)i_c(t_i) \quad (14)$$

$$P_i = \frac{1}{N}\sum_{i=0}^{N-1} T(t_i)\omega(t_i) \quad (15)$$

where, N is the number of simulation points, $v_a(t_i), v_b(t_i)$ and $v_c(t_i)$ are the phase voltages at time of t_i, $i_a(t_i), i_b(t_i)$ and $i_c(t_i)$ are the line currents, $T(t_i)$ and $\omega(t_i)$ are the shaft-torque and the rotational angular-speed, respectively.

2.5 μs of time step is used in the digital computer simulation. Consequently, the system efficiency across the machine is defined as,

$$\eta = \frac{\text{Output power from dc link}}{\text{Input power to the shaft}} \quad (16)$$

$$= \frac{P_o}{P_i} \quad (17)$$

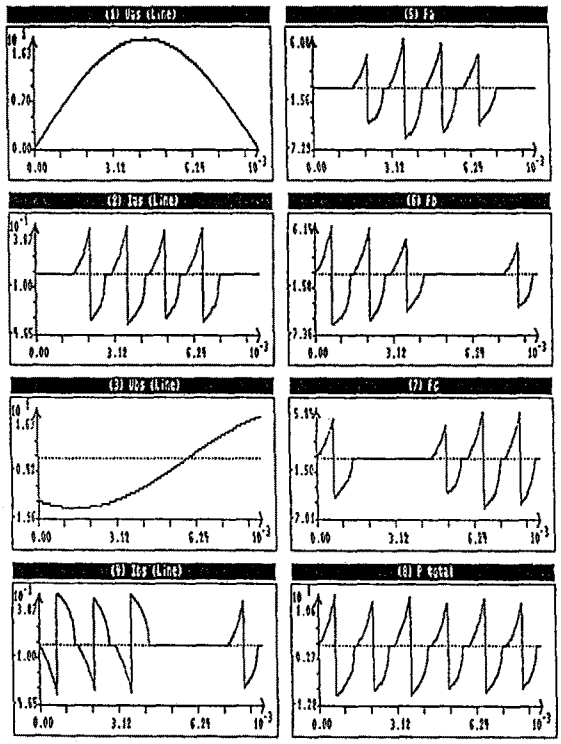

Figure 3. Theoretical results of the scheme

B. Experimental results

The feasibility of the scheme is verified by the comparison of the theoretical and experimental results. The oscillograms of the dc link voltage and current are found in Figure 4(a). With the same time scale at the machine speed of 1800 RPM(1 pu), the instantaneous power waveform is shown in Figure 4(b) which contains the dc link current, too. In power waveform instrumentation, a multiplication chip, XR-2208, is used. The chip has bandwidth of 8-MHz. The dc link current and the attenuated dc voltage are two inputs to the chip, and the power is directly measured at the output pin. From the measured value the actual power is calculated by

$$P_o = k_s k_v k_i \times \text{Measured voltage at chip terminal} \quad (18)$$

where, k_s, k_v and k_i are chip scale factor, voltage gain and current gain, respectively.

Since the voltage is a bipolar quasi-square wave, the instantaneous power waveform is almost a linear expansion of the current in magnitude except polarity change due to the voltage polarity. The oscillations in the power waveform come from the voltage oscillations at the moments of commutation. It is due to the switching of a highly inductive circuit. Figure 4(c) shows the waveforms of phase-voltage and current of the ac mains. The humps in the voltage can be removed by using a low pass filter on the supply side. The bipolarity current explains that only one current path is provided for the field energization and regeneration. In other words, only two phases out of the three phases of the supply

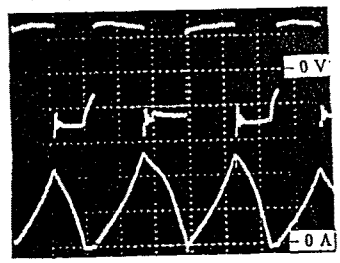

10 V/div
0.2 A/div
0.5 ms/div

(a) Dc link voltage and current

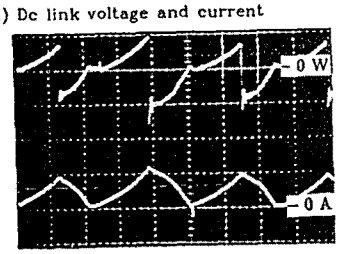

11 W/div
0.5 A/div
0.5 ms/div

(b) Dc link power and current

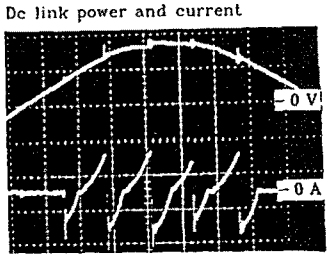

10 V/div
0.5 A/div
1 ms/div

(c) Ac phase voltage and line current

Figure 4. Experimental results of the scheme

are used as the current path at a given time. Two operation modes are discussed in the following using the expanded current and power waveforms.

Motoring mode: As shown in Figure 4(a) a motoring torque is produced by energizing a phase winding during the period when the inductance is increasing. The machine takes power from the ac source up to the point where commutation occurs. The energy taken from the three-phase mains is converted to mechanical output, magnetic field energy and is partly lost in the converter and machine. After the point where commutation occurs, the stored field energy is partly returned to the source, and during this period the front-end converter changes the polarity of the dc link voltage. Some of the field energy is converted to further mechanical output and losses. The converter and machine also take parts of the energy in the form of losses. Experimental measurements of the dc-link current and power in the motoring mode is shown in Figure 5(a), where the net average power is positive.

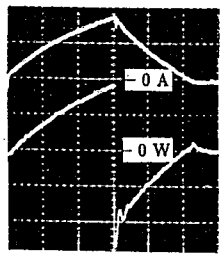

0.2 A/div
4.4 W/div
0.2 ms/div

(a) Winding current and power in motoring mode

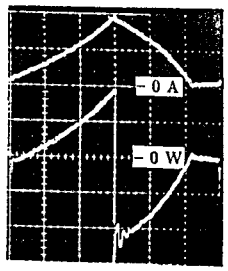

0.2 A/div
4.4 W/div
0.2 ms/div

(b) winding current and power in generation mode

Figure 5. Instantaneous power at DC link

Generation mode: If a phase winding is energized, while the rotor is moving away from the fully aligned position (i.e. during the decreasing inductance), power is generated.

That is, during the generation mode the machine returns power as much as it has taken from the source during the motoring mode. The current takes the shape shown in Figure 5(b), which is a mirror image of Figure 5(a). During the rising current portion, the machine takes energy from the three-phase mains and shaft, and stores energy in the field. During the generation period, the system takes energy from the shaft and returns it to the source.

Figure 6 contains the impacts of the current advancing angle, θ_a on the output power. It depicts the output power on the ideal phase-inductance profiles as a function of rotor position. For dwell angle, $\theta_c = 7°$ and speed of 1800 RPM, power output at dc link are predicted at two voltage levels, $v_{dc} = 0.5$ and 1.0pu. Experimental results have been taken for $v_{dc} = 0.5$pu. The results show that the maximum power is obtained with a significant retarding of θ_a. To maximize the power output, the excitation current should attain its rated value. But, the advance of θ_a more toward the peak inductance with constant θ_c opposes the increase of current. For the given conditions, the system gives the maximum output power around 39° from the unaligned rotor position.

The output power and efficiency at various speed are included in Figure 7, for $\theta_a = 39°$ and $\theta_c = 7°$. The maximum power is predicted and measured near the machine speed of 0.8 pu as shown in Figure 7(a). Decreasing speed reduces the power output of the machine, and in a high speed range the desired current can not be attained due to short rising time and high back-emf. The efficiency shown in Figure 7(b) is almost constant for the entire operating speed range. It can be explained by the comparable losses; copper losses in the low speed range and windage/frictional losses in the high speed range.

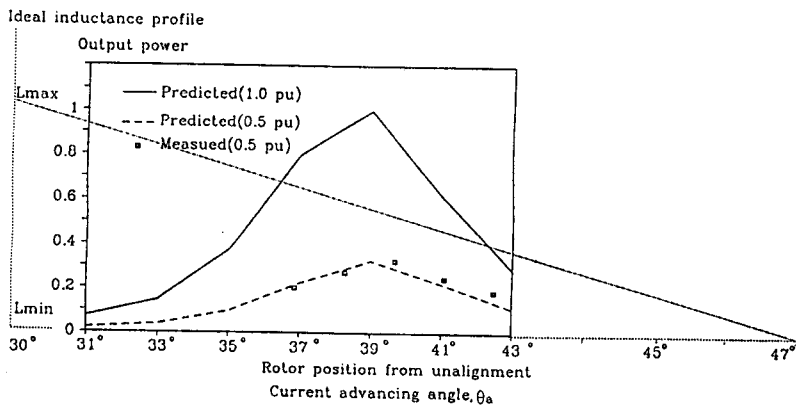

Figure 6. Output power vs rotor position

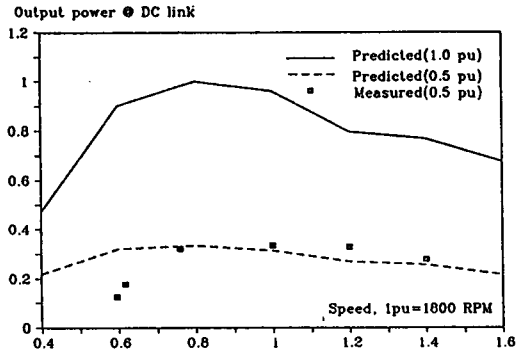

(a) Output power vs. speed for 0.5 and 1.0 pu of Vdc

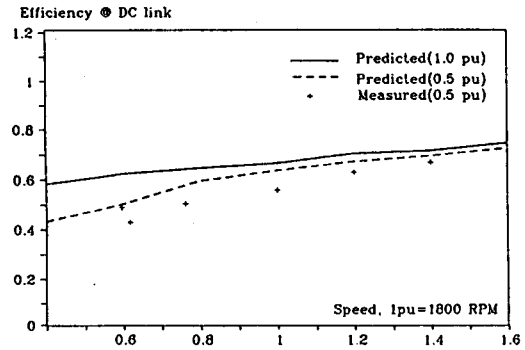

(b) Efficiency vs. speed for 0.5 and 1.0 pu Vdc

Figure 7. Impacts of speed change on output and efficiency

IV. Conclusion

The proposed topology has distinct features such as unidirectional current-flow and bipolarity of dc-link voltage. The topology is able to convert power directly from three-phase ac source to an SRM and vice versa without any dc link capacitor. Through this study, the possible use of SRMs in the VSCF applications is clearly confirmed by the good correlation between the theoretical and experimental results with respect to the following characteristics.

(i) Phase voltage and line current in the ac source.

(ii) Voltage and power in the dc link.

(iii) Relationships between power and efficiency vs speed.

(iv) Relationship between power vs current advancing angles.

Based on these observations, the following original contributions are made in the study of VSCF power conversion scheme with the SRM:

(i) A novel VSCF power conversion scheme with the SRM has been proposed.

(ii) A converter topology with no dc link capacitor have been proposed. This feature enhances the reliability of the power conversion scheme and reduces the weight of the converter system.

(iii) The proposed converter topology directly links the constant frequency ac source to the SRM and they provide for four quadrant operation. This feature makes it attractive for starter-generator applications such as in aerospace, hybrid electric vehicles and remote power stations.

(iv) Various control modes of the proposed scheme have been studied, modeled and analyzed, and experimental correlation is obtained on many key issues.

(v) The feasibility of the proposed VSCF power conversion scheme is demonstrated both by simulation results and experimental verification.

References

[1] R. Krishnan and G. H. Rim, "Modeling, Simulation and Analysis of Variable Speed Constant Frequency Power Conversion Scheme with a Permanent Magnet Brushless DC Generator", IEEE Trans. on Industrial Electronics, Vol. 37, No.4, pp 291-296, August 1990.

[2] R. Krishnan and G. H. Rim, "Design and Operation of Adjustable Power Factor Sinusoidal Converter for Variable Speed Constant Frequency Generation with PMSG", IEEE IAS Conference Record, pp 835-842, Oct. 1989

[3] P.N. Materu and R. Krishnan, "Analytical Prediction of SRM Inductance Profile and Steady-State Average Torque", IEEE IAS Conference Record, Oct. 1990, pp 214-223

[4] P.J. Lawrenson and et al., "Variable-Speed Switched Reluctance Motors", IEE Proc. Vol.127, Pt.B No.4, Jul. 1980, pp 253-265

[5] S.R. MacMinn and W.D. Jones "A Very High Speed Switched Reluctance Starter-Generator for Aircraft Engine Applications", NAECON Proc. May 1989

[6] R.A. Bedingfield, "Development of CAE System for SRM Drive System", M.S. Thesis, Dept of Electrical Engineering, VPI & SU, Blacksburg, VA 24061, Jul. 1991.